The Journal of Headache and Pain

RESEARCH

Open Access

Morphological similarity and white matter structural mapping of new daily persistent headache: a structural connectivity and tract-specific study

Di Zhang[1,5], Fangrong Zong[1,5*], Yanliang Mei[2], Kun Zhao[1,5], Dong Qiu[2], Zhonghua Xiong[2], Xiaoshuang Li[2], Hefei Tang[2], Peng Zhang[2], Mantian Zhang[2], Yaqing Zhang[2], Xueying Yu[2], Zhe Wang[4], Yong Liu[1,5], Binbin Sui[3*] and Yonggang Wang[2*]

Abstract

Background New daily persistent headache (NDPH) is a rare primary headache disorder characterized by daily and persistent sudden onset headaches. Specific abnormalities in gray matter and white matter structure are associated with pain, but have not been well studied in NDPH. The objective of this work is to explore the fiber tracts and structural connectivity, which can help reveal unique gray and white matter structural abnormalities in NDPH.

Methods The regional radiomics similarity networks were calculated from T1 weighted (T1w) MRI to depict the gray matter structure. The fiber connectivity matrices weighted by diffusion metrics like fractional anisotropy (FA), mean diffusivity (MD) and radial diffusivity (RD) were built, meanwhile the fiber tracts were segmented by anatomically-guided superficial fiber segmentation (Anat-SFSeg) method to explore the white matter structure from diffusion MRI. The considerable different neuroimaging features between NDPH and healthy controls (HC) were extracted from the connectivity and tract-based analyses. Finally, decision tree regression was used to predict the clinical scores (i.e. pain intensity) from the above neuroimaging features.

Results T1w and diffusion MRI data were available in 51 participants after quality control: 22 patients with NDPH and 29 HCs. Significantly decreased morphological similarity was found between the right superior frontal gyrus and right hippocampus. The superficial white matter (SWM) showed significantly decreased FA in fiber tracts including the right superficial-frontal, left superficial-occipital, bilateral superficial-occipital-temporal (Sup-OT) and right superficial-temporal, meanwhile significant increased RD was found in the left Sup-OT. For the fiber connectivity, NDPH showed significantly decreased FA in the bilateral basal ganglion and temporal lobe, increased MD in the right frontal

*Correspondence:
Fangrong Zong
fangrong.zong@bupt.edu.cn
Binbin Sui
reneesui@163.com
Yonggang Wang
w100yg@gmail.com

Full list of author information is available at the end of the article

lobe, and increased RD in the right frontal lobe and left temporal-occipital lobe. Clinical scores could be predicted dominantly by the above significantly different neuroimaging features through decision tree regression.

Conclusions Our research indicates the structural abnormalities of SWM and the neural pathways projected between regions like right hippocampus and left caudate nucleus, along with morphological similarity changes between the right superior frontal gyrus and right hippocampus, constitute the pathological features of NDPH. The decision tree regression demonstrates correlations between these structural changes and clinical scores.

Keywords New daily persistent headache, White matter, Structural connectivity, Diffusion MRI, Diffusion tensor imaging

Background

New daily persistent headache (NDPH) is an uncommon headache disorder distinguished by the recurrence of daily headaches shortly after their initiation, usually in patients without a prior headache history [1]. Individuals diagnosed with NDPH can precisely delineate the moment when their headaches first appeared [2]. Previous epidemiological investigations have reported that the prevalence of NDPH in the general population ranges from 0.03 to 0.1% [3, 4]. Although the exact pathogenesis of NDPH remains unknown, the nociceptive transmission of migraine pain has been investigated, and some cortical areas involved in pain perception may affect the whiter matter tracts connecting them [5]. In recent years, neuroimaging studies have been increasingly applied to primary headaches showing, specifically in migraine, widespread white matter abnormalities [6–9]. However, NDPH sometimes presents predominantly with migraine features, which may complicate the diagnosis. Additionally, relatively few studies have investigated NDPH [4, 10, 11]. The association with cortical morphological changes and white matter structural abnormalities from MRI may help to understand the underlying mechanisms of NDPH.

Despite several studies using MRI for NDPH [12–15], there remains a distinct lack of research focusing on the network of anatomically connected regions. At present, two standard approaches are available for imaging anatomical connectivity in humans: structural covariance network (SCN) analysis on T1 weighted (T1w) MRI and tractography from diffusion MRI (dMRI). SCN is a network mapping based on inter-regional similarity of morphometric parameters (i.e. cortical thickness) measured using MRI. It captures cortical structures and is well correlated to cytoarchitecture similarity [16]. While dMRI tractography provides the trajectory of axonal tracts.

For gray matter structural measurements in T1w MRI, previous studies have found some regions with reduced cortical thickness, decreased cortical surface area and different regional gray matter volume in patients with NDPH [12, 13]. However, these findings typically analyze single/several anatomical regions independently without considering associations between brain regions.

For white matter structural descriptions in dMRI, tract-based spatial statistics (TBSS) and diffusion tensor imaging (DTI) along the perivascular space (ALPS) analyses have been applied to investigate the alterations of the white matter microstructure in NDPH [14, 15]. TBSS analysis, which utilized the white matter skeleton, was employed to capture the microstructural abnormalities. Several deep white matter (DWM) tracts exhibited decreased fractional anisotropy (FA), along with increased mean diffusivity (MD) and radial diffusivity (RD) compared with healthy controls [14]. And no significant differences between groups were observed in ALPS index (i.e. the glymphatic function) compared with healthy controls [15]. However, these methods are unable to capture abnormalities in the fiber connections between different brain regions. This is not only because of partial volume effects [17], but also due to the exclusive assessment of the white matter tracts, as they do not focus on the sections connecting each potential pair of regions. In addition, DWM contains long fibers that connect distant areas, which have been extensively studied and well documented, while superficial white matter (SWM) fibers have been often left aside. SWM fibers are short connections which hook-up close-by areas (often neighboring gyri) surrounding the cortex sulci, and they are little known since their small sizes and their proximity to the cortex pose a challenge to study [18]. The SWM abnormalities are found in diseases like Huntington's and Alzheimer's disease and are correlated with cognition function [19–21]. For NDPH, TBSS analysis [14] has shown significant structural changes in the SWM region. However, the lack of support from a better SWM and DWM segmentation method hinders further exploration. Since NDPH involves a chronic pain state, which is related to cortical and subcortical regions. It is necessary to study the SWM structure of patients with NDPH.

For NDPH, the exploration of morphological variations across brain regions, along with the identification of disparities in DTI metrics of interregional fibers and specific tracts, present unexplored opportunities like mechanism research and clinical intervention. In this study, we hypothesized that (1) The gray matter and white matter structures influence each other; (2) patients with NDPH

have considerable gray matter morphological similarities changes compared with healthy controls (HC); (3) NDPHs have meaningful white matter structural changes compared with HCs; and (4) the gray matter and white matter structures can both dominate the prediction of clinical characteristics in NDPHs. The objective of this study was to assess the white matter tracts and interregional structural connectivity changes in patients with NDPH, and their relationship with clinical scores.

Methods

Standard protocol approvals, registrations, and patient consents

The study protocol was approved by the local ethics committee of Beijing Tiantan Hospital, Capital Medical University (number: KY2022-044), and our study was registered on ClinicalTrials.gov (NCT05334927). All participants gave written informed consent.

Demographic data and neuropsychological tests

The cross-sectional MRI study including participants from the headache outpatient unit at Beijing Tiantan Hospital (Capital Medical University). Fifty-four participants, including 24 patients with NDPH and 30 HCs, were consecutively enrolled. The inclusion criteria for patients with NDPH were as follows: (1) NDPH diagnosis based on the International Classification of Headache Diseases, 3rd edition [1]; (2) feasibility of MRI scan; (3) without preventive treatment for at least 3 months; and (4) without the history of excessive use of acute treatment drugs. The general exclusion criteria for patients with NDPH and HCs were as follows: (1) combined with other types of primary headache and pain disorders; (2) pregnancy or breastfeeding; (3) combined with other neurological, cardio-cerebrovascular, and endocrine system diseases; (4) any drug or alcohol abuse history; (5) first degree relative with headaches; and (6) significant brain lesions or white matter hyperintensities (Fazekas score > 1, especially at the level of the lateral ventricular body). For the MRI data of all 54 enrolled subjects, two experienced neuroradiologists visually checked them to exclude three subjects with incomplete brain structure scans.

Demographics, body mass index (BMI), headache disease duration (years), clinical scores including Visual Analogue Scale (VAS), Headache Impact Test-6 (HIT-6) scores, Patient Health Questionnaire-9 (PHQ-9) scores, Generalized Anxiety Disorder-7 (GAD-7) scores, Pittsburgh Sleep Quality Index (PSQI) scores and Montreal Cognitive Assessment (MoCA) scores were collected in patients with NDPH. The VAS allows patients to self-report the perceived intensity of their pain, where a higher score indicates greater pain [22]. And the HIT-6 questionnaire evaluates the wide burden of headache, with higher scores indicating greater impact on the daily life of the respondent [23]. The score of PHQ-9 is commonly used to screen for depression with a recommended cut-off score of 10 [24]. The scores of 10 or higher on the GAD-7 indicates generalized anxiety disorder [25]. The PSQI score is used to evaluate the quality and patterns of sleep and poor quality is defined when it ≥ 7 [26]. And the MoCA score < 26 indicates that the participant has some degree of cognitive impairment [27].

MRI acquisition

All participants underwent brain MRI on a 3T GE MR scanner (Signa Premier, GE Healthcare) with a 48-channel head coil. The participants were instructed to remain motionless with their eyes closed during the MRI acquisition. The T1w images were acquired by using the magnetization-prepared rapid gradient echo (MPRAGE) echo sequence (echo time (TE) = 2.96 ms, repetition time (TR) = 1983.81 ms, inversion time (TI) = 880 ms, flip angle = 8°, field of view 250 mm, resolution = $1.0 \times 1.0 \times 1.0$ mm^3), and the diffusion-weighted images were acquired by using the spin-echo EPI sequence (TE = 85 ms, TR = 5285 ms, field of view 208 mm, resolution = $2.0 \times 2.0 \times 2.0$ mm^3. The dMRI data include 9 images of b = 0, 50 gradient directions with a b-value of 1000 s/mm^2 and 50 gradient directions with 2000 s/mm^2 under the anterior-to-posterior phase encode direction, and include 4 images of b = 0 and 3 gradient directions with 2000 s/mm^2 under the posterior-to-anterior phase encode direction.

Imaging analysis

The pipeline of imaging analysis was shown in Fig. 1. The T1w and dMRI data were firstly preprocessed, then with the goal of studying interregional connectivity, we constructed connectivity matrices weighted by DTI metrics and morphological similarities. The DTI metrics weighted connectivity matrices were generated from the whole brain tractograms. The regional radiomics similarity networks (R2SN) [28] were built from T1w MRI. Specifically, R2SN is a type of SCN. Compared with simple SCN methods, R2SN utilizes more morphological variables and captures finer structural changes. In addition, we employed a new method anatomically-guided superficial fiber segmentation (Anat-SFSeg) [21] to segment SWM and DWM fiber tracts and then identified the tract-specific alterations. Finally, the tract-based analysis was performed after fiber segmentation, and matrices-based analysis was generated from the fiber connectivity matrices and R2SN construction.

Tract-based analysis

Diffusion weighted images were preprocessed using MRtrix3 [29]. Briefly, for each scan, diffusion images

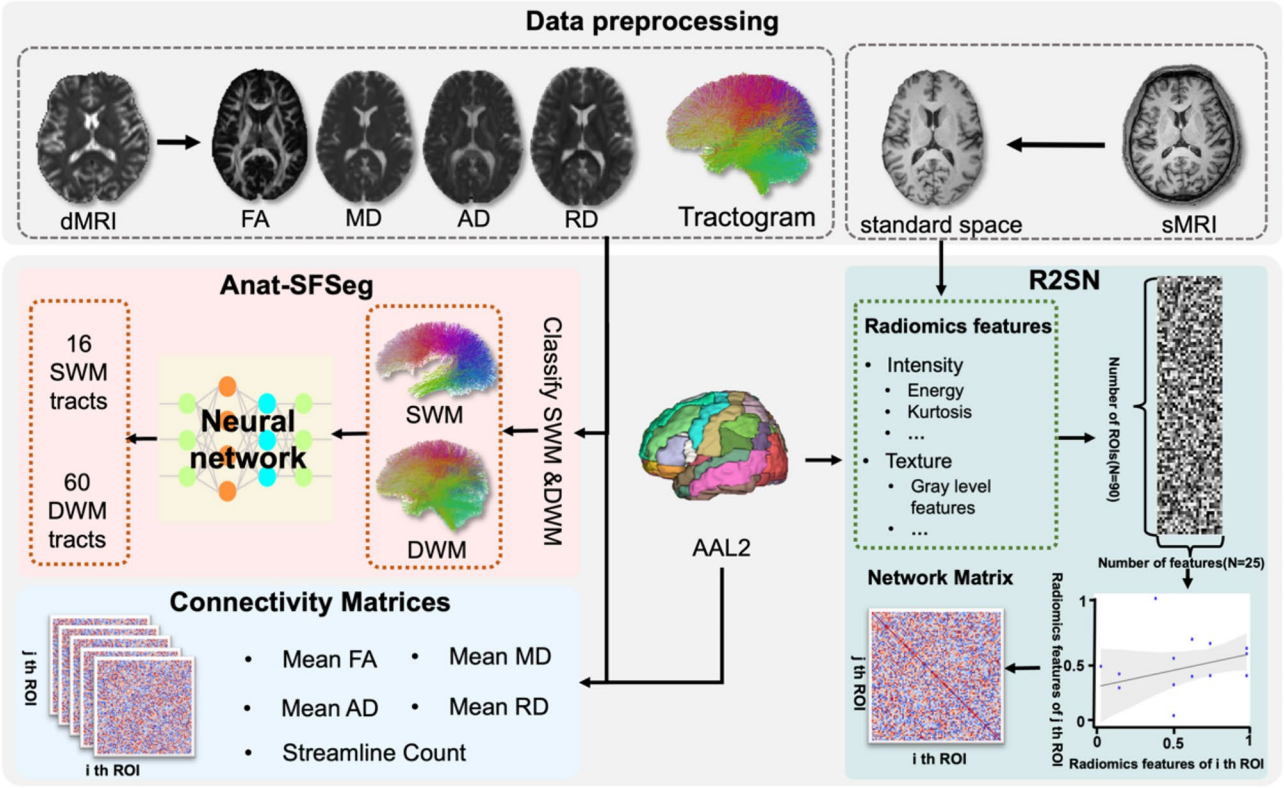

Fig. 1 The framework contains data preprocessing and data analyses. Diffusion MRI (dMRI) data were preprocessed to generate the fractional anisotropy (FA), mean diffusivity (MD), axial diffusivity (AD), and radial diffusivity (RD) maps and the whole-brain tractograms, and T1-weighted (T1w) MRI were preprocessed and registered to standard space. The data analyses include fiber segmentation, fiber connectivity matrices and regional radiomics similarity networks (R2SN) construction. The whole brain tractograms were segmented into superficial white matter (SWM) and deep white matter (DWM) tracts by anatomically-guided superficial fiber segmentation (Anat-SFSeg) method, and five fiber connectivity matrices were generated using the anatomical automatic labeling (a second version, AAL2) atlas. For R2SN construction, 25 radiomics features of each brain region in T1w MRI were first extracted, then the Pearson's correlations between these features of paired brain regions were calculated, which formed a matrix named R2SN

were denoised (*dwidenoise* in MRtrix3 [30]), Gibbs ringing correction (*mrdegibbs* in MRtrix3 [31]), head motion correction, eddy current-induced and inhomogeneity distortion correction (*dwifslpreproc* [32–35] and *dwibiascorrect* [36] in MRtrix3), b=0 reference image creation by averaging all images with no gradients. The diffusion tensor was fitted using the same toolbox, and FA, MD, RD, and AD maps were generated (*dwi2tensor* in MRtrix3 [37, 38]). For T1w MRI, firstly we striped the skulls by the Brain Extraction Tool [39] in Oxford Centre for Functional MRI of the Brain Software Library 6.0 (FSL6.0) [40], then the images were registered to the O'Donnell Research Group (ORG) space [41] using symmetric normalization in Advanced Normalization Tools [42]. Cortical parcellation was obtained based on the Desikan-Killiany Atlas [43], and the subcortical parcellation from a white matter atlas [44] was achieved by *recon-all* in FreeSurfer7.4.1 [45, 46]. Subsequently, the b=0 reference image was registered to the T1w images using the FMRIB's Linear Image Registration Tool in FSL6.0, and this transform was applied to register the preprocessed diffusion data.

After the data preprocessing, the fiber orientation distribution (FOD) was estimated using the constrained spherical deconvolution method [47]. The probabilistic whole-brain tractography method second-order integration over FOD [48] was conducted to generate the whole brain tractograms. The tractography settings were used: step size=1 mm; maximum angle theta between successive steps=45°; minimum length of any track=10 mm; maximum length of any track=200 mm; FOD amplitude cutoff threshold for terminating tracks=0.1. Finally, the whole brain tractograms were also registered in ORG space using the unbiased groupwise registration method [49].

Using an advanced point-cloud-based neural network Anat-SFSeg [21], the whole brain tractogram was segmented into 800 fiber clusters including both SWM (198 clusters) and DWM (602 clusters), which are based on the ORG Fiber Clustering White Matter Atlas [41] (https://github.com/SlicerDMRI/ORG-Atlases). Guided by the cortical and subcortical brain regions from T1w MRI using FreeSurfer7.4.1 [45, 50], Anat-SFSeg performed best in segmenting these fiber clusters. Specifically,

Anat-SFSeg consisted of a unique fiber anatomical descriptor as well as a deep learning network based on point-cloud data. The fiber anatomical descriptor was generated by mapping the whole brain fibers to the cortical and subcortical brain regions. And the spatial coordinates of the fibers, represented as point clouds, alongside the anatomical descriptor were fed into the neural network. This network was trained using high-quality data from the 100 participants in the Human Connectome Project. For inference, firstly, the stage-one pre-trained models were used on the clinical data to classify SWM and DWM [51], then they were accurately segmented to 198 and 602 clusters through the Anat-SFSeg's pre-trained weights respectively. For SWM, the 198 clusters were further composed into 16 categories in the left and right hemispheres according to their anatomical locations. And for DWM, 602 clusters were further combined into 60 categories. Finally, DTI metrics were extracted, and the average FA, MD, RD, and AD values were calculated along these categories.

Matrices-based analysis

For dMRI, several fiber connectivity matrices weighted by mean FA, mean MD, mean AD, mean RD, and streamline count were generated from the whole brain tractograms. Streamline, which is the reconstructed fiber and is a more geometric term formed by connecting many three-dimensional point coordinates. These matrices were 90 ×90 because they were generated between each pair of subregions of the anatomical automatic labeling (a second version, AAL2) atlas [52], which contains 90 subregions in the bilateral cerebrum. Two regions A and B were considered to be connected with each other if one or more streamlines terminated in region A also terminated in region B.

For T1w MRI data, R2SN [28] was generated for each participant to depict the morphological similarity between different brain regions. Specifically, the radiomics features for each brain region defined in the AAL2 atlas were extracted. The definitions and detailed descriptions of these radiomics features can be found in previous publications [53–55]. Briefly, the subregions' radiomics features were extracted using the *pyradiomics* tool [56], and 25 features including both intensity and texture features were retained after selection. The intensity features include energy, kurtosis, mean absolute deviation, skewness, entropy, etc. The textural features contain autocorrelation, cluster prominence, cluster shade, cluster tendency, high gray-level run-length emphasis, and high gray-level long run-length emphasis, among others. The specific radiomics features analyzed in this study were based on those described in the previous research [28]. Finally, the R2SN was established by calculating the Pearson's correlations of the pairwise interregional normalized features.

Statistical analyses

Demographic characteristics were compared by applying two-sample unpaired t-tests for continuous variable which belongs to normal distribution (BMI) and Mann-Whitney test for skewed distribution (age), and chi-squared test for the qualitative variable (sex), respectively. For tract-based analysis, the average DTI metrics for the 16 SWM and 60 DWM fiber categories were extracted to test the differences between NDPH and HC. The 2-sample unpaired t-tests of FA, MD, RD, and AD metrics for each fiber category were conducted, with adjustment for age and sex variables. The tract-based results were considered significant at corrected $p<0.05$ after Bonferroni multiple comparisons. For matrices-based analysis, each participant contains six 90×90 matrices. For the five fiber connectivity matrices, we utilized the network-based statistic (NBS) approach [57] to make multiple comparisons thus to identify significant fiber connections between the patients and HCs using Gretna software [58](http://www.nitrc.org/projects/gretna). The analysis was conducted with edge-wise t-tests, applying an edge-level significance threshold of $p<0.005$. Statistical significance was determined after 5,000 permutations, and subnetworks with a corrected component-level $p<0.05$ were considered statistically significant. For R2SN, we conducted Bonferroni multiple comparisons on the edge-wise t-test results, and the connection with a corrected $p<0.05$ was considered statistically significant.

Feature importance for predicting clinical characteristics

To explore the associations between the neuroimage features extracted above and clinical characteristics (headache history (years), VAS, HIT-6, GAD-7, PHQ-9, PSQI and MoCA scores), the decision tree regression was utilized to predict these clinical characteristics by inputting age, sex and statistically inter-group significant neuroimaging features. Decision tree regression is a machine learning technique that predicts the value of a target variable by learning simple decision rules inferred from the data features [59]. Instead of assuming a causality between variables, and works by recursively partitioning the data based on the most meaningful feature that best separates the target variable. One key aspect of decision tree regression is its ability to assess the importance of independent variables in predicting the target variable. By evaluating how much each variable contributes to reducing the variance in the target variable, decision tree regression can prioritize and highlight the significance of different features in the prediction process. Due to the overfitting phenomenon caused by small sample size, we took some measures as following. (1) We used 5-fold

cross-validation to train and test the model; (2) We tried to control the complexity of the decision tree through parameter settings; (3) Through multiple experiments, we chose the model that minimized the mean squared error between the predicted value and the true value.

Results

Demographic and neuropsychological characteristics

Two experienced neuroradiologists visually checked the scans and found that 3 subjects (1 HC and 2 patients with NDPH) had missing parietal lobes in dMRI data, ultimately leaving 51 participants for the study, including 22 patients with NDPH and 29 HCs. They all underwent T1w and diffusion MRI, and their characteristics are included in Table 1. All participants had demographics and BMI scores, and all participants with NDPH had headache disease duration (years) and VAS scores. Other indicators were only present in some patients with NDPH. Other patients were in discomfort or experiencing a headache episode during the assessment, which affected their ability to complete the scales. No significant differences were found in age, sex, BMI between patients and HCs.

Table 1 Baseline Participant Characteristics

	Control cohort ($n=29$)	NDPH cohort ($n=22$)	*p* value
Age, y	32.0 (9.2)	39.8 (21.6)	0.123(distinct variance)
BMI	22.1 (2.9)	23.8 (4.1)	0.114(equal variance)
Sex, female/male	17/12	11/11	0.54
Headache disease duration (years)	—	[1,15] (13.2)	—
Pain intensity VAS score	—	4.9 (2.0)	—
HIT-6 score [a]	—	61.1 (11.2)	—
PHQ-9 score [b]	—	9.9 (6.7)	—
GAD-7 score [c]	—	7.5 (5.6)	—
PSQI score [d]	—	9.4 (4.4)	—
MoCA score [e]	—	21.6 (6.5)	—

Abbreviations BMI=body mass index; HIT-6=Headache Impact Test-6; MoCA=Montreal Cognitive Assessment; NDPH=new daily persistent headache; PHQ-9=Patient Health Questionnaire-9; PSQI=Pittsburgh Sleep Quality Index; VAS=Visual Analogue Scale

Mean (SD) for variables that follow normal distributions. The distribution of headache history (years) doesn't follow a normal distribution, we show the interquartile range (SD). The age range of the control cohort is 21 to 59 years old, and that of the NDPH cohort is 12 to 80 years old

[a] The NDPH cohort included 16 participants with HIT-6 score

[b] The NDPH cohort included 17 participants with PHQ-9 score

[c] The NDPH cohort included 17 participants with GAD-7 score

[d] The NDPH cohort included 16 participants with PSQI score

[e] The NDPH cohort included 10 participants with MoCA score

Tract-based analysis

The percentage changes of DTI metrics in population-mean SWM were shown in Fig. 2, as well as several fiber tracts with distinctly differences in FA and RD between NDPH and HC groups. As observed, there were widespread abnormalities in the RD and FA maps. And the differences of FA in SWM fiber tracts between NDPH and HC were statistically significant after multiple comparisons (uncorrected $p<0.05/16$). However, there were no significant differences in MD and AD after multiple comparisons. The statistical results of all 16 SWM fiber tracts can be found in the supplementary materials (Result S1).

The significance of the differences among the 16 fiber tracts was not consistent. The SWM showed decreased FA on the right superficial-frontal (Sup-F), left superficial-occipital (Sup-O), bilateral superficial-occipital-temporal (Sup-OT), right superficial-temporal (Sup-T), and increased RD in the left Sup-OT. There were no significant group differences between the AD and RD values in the SWM.

For DWM, since there were no significant results after multiple comparisons (uncorrected $p<0.05/60$), some tract results that changed before multiple comparisons are presented. For example, patients with NDPH showed lower FA than HC on the right arcuate fasciculus (AF), right striato-frontal (SF) and left thalamo-occipital (TO). Higher RD values were found on the left AF, right uncinate fasciculus (UF) and left superior longitudinal fasciculus III (SLF-III). The statistical results of all DWM fiber tracts could be found in the supplementary materials (Result S1). For illustration, the changes of DTI metrics of these fiber tracts between NDPH and HC are shown in Fig. 3.

Matrices-based analysis

There were six 90×90 matrices including mean FA, MD, AD, RD, streamline count and R2SN for each participant. The edge-wise t-tests with Bonferroni correction were conducted to precisely locate the significantly different connections of R2SN structural-based matrix. The NBS approach was used to identify the distinct connected subnetwork with varying diffusion-based (mean FA, MD, AD, RD and streamline count) matrices between the patients and HCs. Significantly decreased similarity in R2SN between the right superior frontal gyrus (medial orbital) and right hippocampus was found in NDPH compared to HC (corrected $p<0.05$). For the structural connectivity analysis, patients with NDPH showed a significantly decreased component of FA values in the bilateral basal ganglion and temporal lobe, a significantly increased component of MD values in the right frontal lobe, and a significantly increased component of RD values in the right frontal lobe and left temporal-occipital

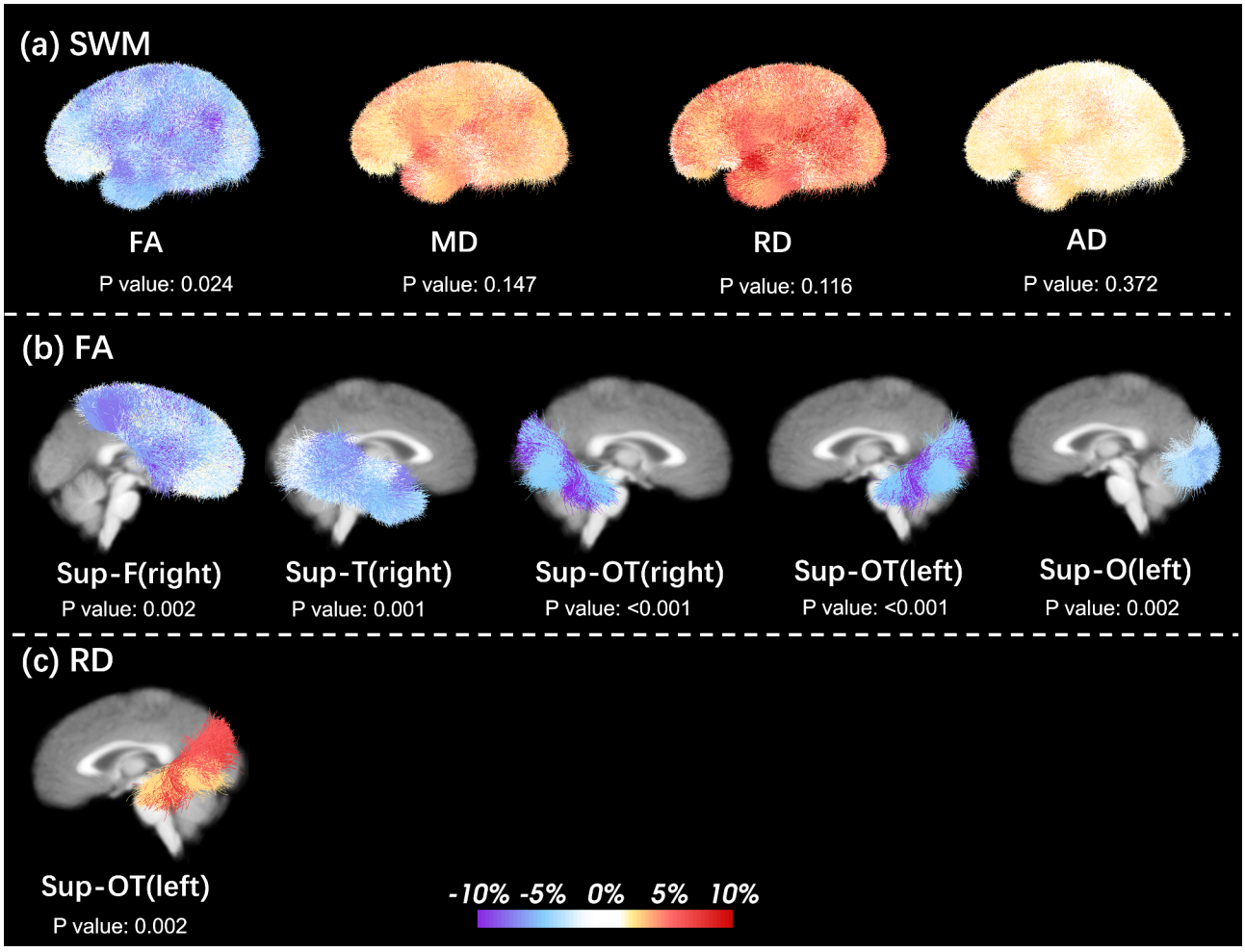

Fig. 2 Percentage change in population mean superficial white matter (SWM), and several fiber categories with significant differences in FA and RD between new daily persistent headache (NDPH) and healthy controls (HC) after multiple comparisons. The uncorrected p values are added under each fiber tract. In (**a**), the population-mean SWM percentage change maps show the differences between NDPH and HC. And several tracts with significant differences in FA and RD between groups were shown in (**b**) and (**c**). The term 'NDPH-HC' refers to the average diffusion tensor metrics of each cluster in all patients with NDPH minus the average metrics of each cluster in all HCs. Red indicates an increase in percentage, while blue indicates a decrease. (Abbreviations: AD = axonal diffusivity, MD = mean diffusivity, FA = fractional anisotropy, RD = radial diffusivity, Sup-F = superficial frontal, Sup-O = superficial occipital, Sup-OT = superficial occipital-temporal, Sup-T = superficial temporal.)

lobe (corrected $p<0.005$). And no significant connections were found in AD and streamline count matrices. The connections with significant differences between NDPH and HC are shown in Fig. 4; Table 2.

Feature importance for predicting clinical characteristics

Decision tree regression can prioritize and highlight the significance of different features in the prediction process. Given that input variables include imaging and non-imaging features, an importance value of greater than 50% for neuroimage features was considered to have a considerable influence on predicting clinical characteristics in this study. For SWM fiber tracts, we have identified the neuroimage features which the importance values are than 0.5, as shown in Fig. 5(a). And for the fiber connectivity and R2SN matrices, the connections that predominantly influence the prediction of specific clinical characteristics are shown in Fig. 5(b).

In Fig. 5 (a), most SWM fiber tracts, previously found to have significant inter-group differences, could predominantly guide the prediction of clinical characteristics. Additionally, DTI metrics of some fiber tracts made considerable contributions to the prediction of clinical scores. For example, the importance of the FA of Sup-F in the right hemisphere for predicting HIT-6 reached 0.78. In Fig. 5 (b), for the DTI and R2SN matrices, connections with significant inter-group differences showed varying importance for different clinical scores. For example, in the FA connectivity matrix, the connection from the right hippocampus to the left caudate nucleus had a stronger influence in predicting MoCA, while it had a slightly lesser impact on predicting other clinical scores.

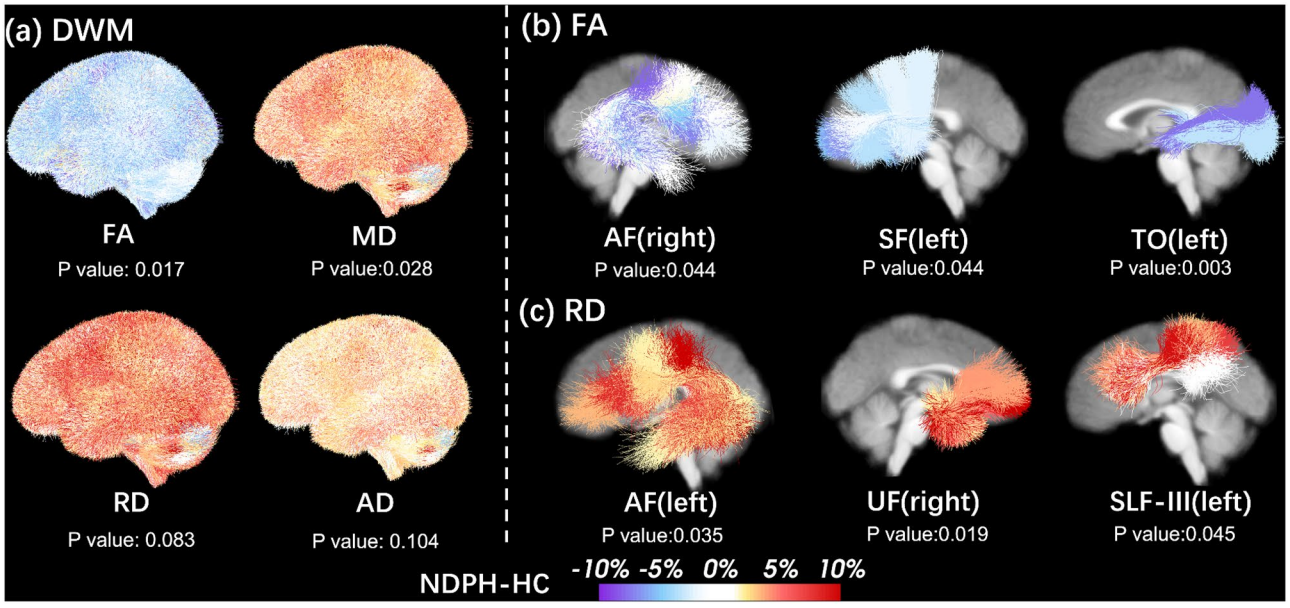

Fig. 3 Percentage change in population mean deep white matter (DWM), and several fiber categories with significant differences before multiple comparison in FA and RD between new daily persistent headache (NDPH) and healthy controls (HC) before multiple comparisons. The uncorrected p values are added under each fiber tract. In the left, the population-mean DWM percentage change maps show the differences between NDPH and HC. And several tracts with significant differences before multiple comparison in FA and RD between groups were shown in the right. The term 'NDPH-HC' refers to the average diffusion tensor metrics of each cluster in all patients with NDPH minus the average metrics of each cluster in all HCs. Red indicates an increase in percentage, while blue indicates a decrease. (Abbreviations: AD = axonal diffusivity, AF = arcuate fasciculus, FA = fractional anisotropy, MD = mean diffusivity, RD = radial diffusivity, SF = striato-frontal, SLF-III = superior longitudinal fasciculus III, TO = thalamo-occipital, UF = uncinate fasciculus.)

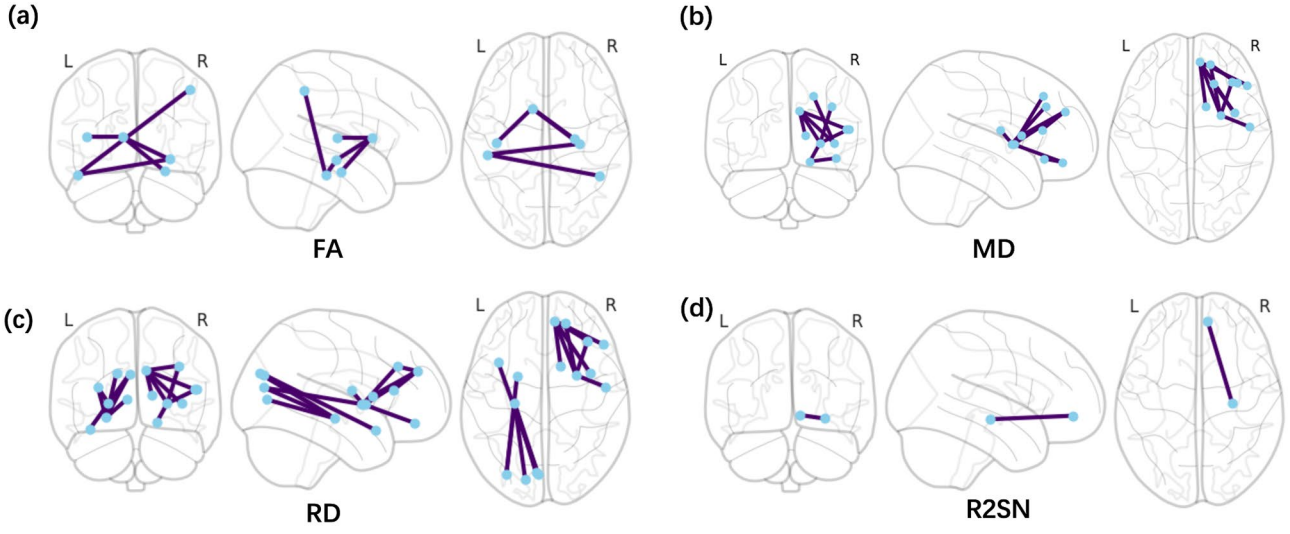

Fig. 4 The connections with significant difference between new daily persistent headache (NDPH) and healthy controls (HC). The matrices-based analysis was conducted to precisely locate the significantly different connections of diffusion-based structural connectivity matrices and the regional radiomics similarity network (R2SN). (Abbreviations: FA = fractional anisotropy, MD = mean diffusivity, RD = radial diffusivity)

Discussion

In this study, we found considerable changes in interregional morphological similarity and white matter structural abnormalities in patients with NDPH using both T1w and diffusion MRI. The white matter structure differences were generated through both fiber connectivity matrices and tract-specific studies. And the results revealed that patients with NDPH exhibited significantly morphological similarity decreased in subregions, and decreased FA, increased RD of specific white matter structure compared to HC.

Diffusion MRI tractography, which generates three-dimensional streamlines, offers a noninvasive method for fiber connectivity mapping. This method provides a

Table 2 Connections with significant changes in patients with NDPH compared to healthy controls in gray matter and white matter structural connectivity

Matrices	Change	Brain regions connected	*P* value (uncorrected)
Mean FA weighted matrix	Decreased	Right Hippocampus-Left Caudate nucleus	0.005
		Right Hippocampus-Left Inferior temporal gyrus	0.002
		Right Parahippocampal gyrus- Left Caudate nucleus	0.003
		Right Angular Gyri-Left Inferior temporal gyrus	0.003
		Left Caudate nucleus-Left Heschl gyrus	< 0.001
Mean RD weighted matrix	Increased	Left Hippocampus-Left Calcarine fissure	0.001
		Left Hippocampus-Left-Cuneus	0.001
		Left Hippocampus-Left Superior occipital gyrus	< 0.001
		Left Hippocampus-Left-Middle occipital gyrus	0.002
		Left Cuneus-Left Superior Temporal gyrus	0.002
		Left Middle occipital gyrus-Left Lenticular nucleus putamen	0.003
		Right Middle frontal gyrus -Right Lenticular nucleus putamen	< 0.001
		Right Middle frontal gyrus-Right Superior frontal gyrus	0.002
		Right Middle frontal gyrus-Right Lenticular nucleus putamen	0.001
		Right Inferior frontal gyrus (triangular part)-Right Superior frontal gyrus	0.001
		Right Rolandic operculum-Right Lenticular nucleus putamen	0.001
		Right Superior frontal gyrus-Right Insula	< 0.001
		Right Superior frontal gyrus-Right Caudate nucleus	0.004
		Right Superior frontal gyrus-Right Lenticular nucleus putamen	0.002
Mean MD weighted matrix	Increased	Right Superior frontal gyrus (dorsolateral)-Right Insula	0.002
		Right Middle frontal gyrus (orbital part)-Inferior frontal gyrus (orbital part) Right	0.002
		Right Middle frontal gyrus (orbital part)-Right Lenticular nucleus putamen	< 0.001
		Middle frontal gyrus Right-Right Lenticular nucleus putamen	0.001
		Right Inferior frontal gyrus (triangular part)-Right Superior frontal gyrus (medial)	0.002
		Right Rolandic operculum-Right Lenticular nucleus putamen	< 0.001
		Right Superior frontal gyrus (medial)-Right Insula	< 0.001
		Right Superior frontal gyrus (medial)-Right Caudate nucleus	0.001
		Right Superior frontal gyrus (medial)-Right Lenticular nucleus putamen	0.001
R2SN	Decreased	Right Superior frontal gyrus (medial orbital)-Right Hippocampus	< 0.001

Abbreviations FA = fractional anisotropy; MD = mean diffusivity; R2SN = regional radiomics similarity networks; RD = radial diffusivity

direct anatomical relationship within white matter, both in whole-brain tractogram-based connections and in fiber tracts obtained through advanced segmentation methods. An increase in MD, reflecting greater water molecule diffusion, is often associated with tissue atrophy. Increased AD is related to axonal atrophy, while increased RD indicates reductions in myelination [60]. Decreased FA suggests loss of water directionality, likely due to structural damage [61]. Notably, the relationships between DTI metrics and white matter pathologic features are interpreted but not completely clear, the researchers should be cautious [62].

For white matter structure, the SWM in NDPH showed decreased FA in right Sup-F, left Sup-O, bilateral Sup-OT, right Sup-T, and increased RD in left Sup-OT. These findings indicate significant structural abnormalities in the SWM of patients with NDPH. The right Sup-F was involved in higher cognitive functions and emotional regulation [63], suggesting that the emotional dysregulation observed in patients with NDPH. The left Sup-O and bilateral Sup-OT were associated with visual processing and integration, which may link visual stimuli to pain perception pathways, potentially exacerbating headache symptoms [64]. The right Sup-T was crucial for auditory and language processing, and its impairment could influence how patients perceive and respond to auditory information, further affecting their pain experience [64, 65]. Increased RD in the left Sup-OT may reflect demyelination or other structural damage, which could disrupt the normal processing of visual and emotional stimuli, contributing to the chronic pain and emotional distress characteristic of NDPH. Overall, the observed SWM abnormalities in these regions highlight their role in pain perception and emotion regulation, underscoring the impact of white matter structure on the pathophysiology of NDPH. Notably, the findings shown in Figs. 2 and 3 are not consistent. This means that for the same fiber tract, there was a significant decrease in FA, but there was no obvious increase in diffusivity. This is a common phenomenon and some reasons are as follows: (1) FA values are lower in complex fiber architecture because the directionality of diffusion on the voxel-scale is lower, which

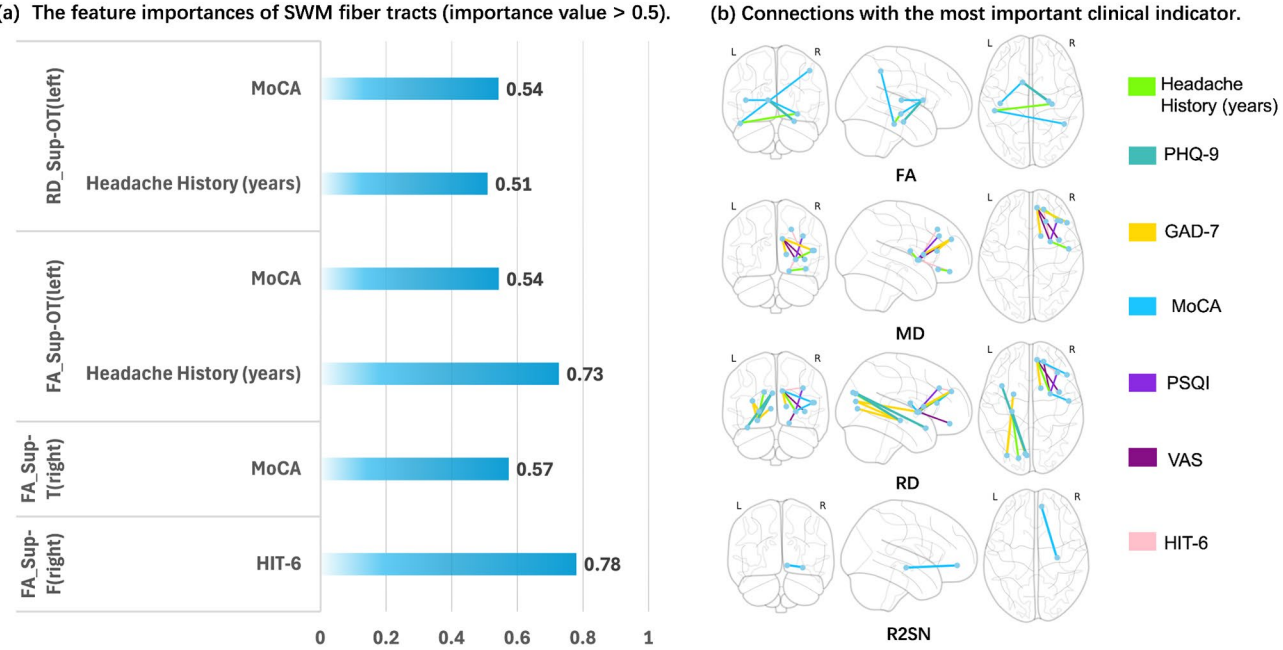

Fig. 5 The dominance of neuroimaging features for predicting clinical characteristics. The feature importance values greater than 0.5 of different superficial white matter (SWM) fiber tracts are shown in Fig. 5 (**a**), and the connections that predominantly influence the prediction of specific clinical characteristic are shown in Fig. 5(**b**)

leads to a decrease in diffusivity [66]; (2) The statistical tests we conducted were adjusted with age and gender, which influenced the diffusivity parameters independently; (3) There might be errors in the estimation of diffusion tensor metrics.

The neural circuits implicated by white matter projections fibers were crucial for understanding potential mechanisms underlying NDPH, particularly those associated with pain perception, emotional processing, cognition and sleep quality. According to our results, the significant changes in FA, RD, and MD metrics across various white matter tracts suggest that connection disruptions between caudate nucleus, hippocampus, and cortical regions (mainly frontal, temporal, and occipital lobe) could play a pivotal role in the pathophysiology of NDPH. For instance, the decreased FA between the right hippocampus and left caudate nucleus, as well as other regions like the right inferior temporal gyrus and the right Angular gyri, indicate impaired connectivity within circuits involved in memory and auditory processing [67]. These alterations might affect how patients perceive and process sensory information, potentially heightening their pain sensitivity [68]. Studies show that stimulation of the caudate nucleus reduced pain reactivity by decreasing the emotional response to pain without affecting motor activity or arousal levels [69]. Our study found structural damage in the neural projection pathways between the bilateral caudate nucleus and frontal and temporal lobes. This suggests weakened neural connections between the caudate nucleus and these brain regions, potentially contributing to persistent pain and emotional responses in NDPH patients. Similarly, the increased RD observed between the left hippocampus and occipital regions, including the calcarine fissure and the superior occipital gyrus, points to demyelination or other structural damage in pathways critical for visual processing. This disruption could interfere with how visual stimuli are integrated and interpreted, which may exacerbate headache symptoms through heightened sensory sensitivity or misprocessing.

The increased MD in connections involving the right superior frontal gyrus and insula suggests broader structural abnormalities affecting regions integral to emotional regulation and pain modulation [70]. The superior frontal gyrus and insula are known to play important roles in the cognitive and affective dimensions of pain [68]. Disruptions in these areas could contribute to the emotional dysregulation and altered pain perception frequently reported by patients with NDPH. Moreover, the significant decrease in R2SN between the right superior frontal gyrus (medial orbital) and right hippocampus further support the involvement of these regions in the neural mechanisms of NDPH. The superior frontal gyrus and hippocampus are both related to cognitive functions and particularly to working memory [71, 72]. In previous studies, it has been shown that interregional morphological similarity changes in R2SN reflected imperceptible structural changes. And the changes were associated with cognition in patients with Alzheimer's disease and mild cognitive impairment [73–75]. Therefore, in this study,

the changes of morphological similarity in these regions suggest that cognition of patients may be affected.

In addition, the importance scores of neuroimaging features from fiber tracts and matrices were calculated using decision tree regression, which is a robust and effective machine learning technique well-suited for modeling the relationships between clinical scores and neuroimage features [59]. The analysis revealed that the DTI metrics of several SWM tracts, including the right Sup-F, right Sup-T and left Sup-OT, are crucial for predicting different clinical scores. Specifically, FA of the right Sup-F tract demonstrated a high importance score for predicting HIT-6 scores, indicating its significant role in assessing the impact of headaches on daily life. Moreover, the results indicated that FA changes in the Sup-OT are more closely related to the duration of headache history, reflecting the progressive nature of NDPH. The connectivity matrix analysis further emphasized that specific brain region connections are key predictors of clinical scores. For example, the FA connectivity matrix showed that the connection from the right hippocampus to the left inferior temporal gyrus predicts MoCA scores well, suggesting its association with cognitive functions in patients with NDPH. Overall, our findings underscore the importance of specific SWM tracts and inter-regional connections in understanding the neural mechanisms underlying NDPH, and offer potential biomarkers for predicting clinical outcomes. Decision tree regression is able to capture more possible correlations compared to the simple partial correlation. At the same time, its results were also significantly correlated with the correlation coefficients obtained by simple partial correlation (as shown in supplementary materials Result S3). In addition, compared with traditional multiple linear regression, the decision tree regression has more advantages like strong interpretability and greater robustness to outliers. However, in this work, due to the small sample size, the model was prone to overfitting. Many experiments need to be conducted to select the most suitable model, which is not as convenient as multiple linear regression.

In summary, our findings suggest that abnormal SWM structure in the frontal, temporal, and occipital lobes, along with damage to neural projection pathways within these regions, constitutes a pathological feature of NDPH. These abnormalities likely disrupt the integration of sensory information, emotional responses, and cognitive processes, thereby contributing to the onset and maintenance of chronic headache symptoms in patients with NDPH. Notably, the fiber connectome provides fine connections between individual brain regions, while fiber tracts offer a coarser view. So the results of both the DTI matrices-based and tract-based analyses are complementary. Understanding these alterations provides valuable insights into the neural mechanisms underlying NDPH and may guide the development of targeted therapeutic interventions.

The present study has several limitations and offers prospective avenues for further research. First, the study was a cross-sectional design research, which limits our ability to assess the causalities between neuroimaging features and clinical scores. The longitudinal data will be acquired and studied in the future. Second, given the rarity of the disease, the number of participants we were able to recruit was limited. Despite the limited sample size, the results still showed noticeable differences. In the future, we plan to recruit more participants to provide a more comprehensive assessment of these differences. Third, the metrics we have discussed, whether they are tract-based or matrices-based, are considered as the first-order indicators. While the second-order indicators, i.e. the network properties, equally need to be further explored. Fourth, we only used the DTI model combined with a white matter segmentation algorithm to explore the abnormalities of white matter structure in NDPH, which has not been studied before. Since high b-value data were acquired, it is possible to apply other more complex models such as diffusion kurtosis imaging, neurite orientation dispersion and density imaging models in future research. Fifth, the coordinate system in this study is ORG space because the fiber tracts atlas is in this space. Although the coordinate origin of ORG is very close to the commonly used MNI space, this will hinder the promotion of the method. Sixth, we primarily focused on cerebral other than cerebellum. Since cerebellum also plays an important role in pain modulation, we plan to explore the role of cerebellum in NDPH in future studies. Finally, our study relied on T1w and dMRI data, which may not capture all aspects of brain pathology associated with NDPH. Incorporating other imaging modalities such as functional MRI or positron emission tomography could provide a more comprehensive understanding of the underlying neural mechanism.

Conclusions

The morphological similarity and white matter structural abnormalities open a window into the pathogenesis of NDPH. Our research indicates that the damage to SWM structure, along with neural projection pathways within some brain regions, constitute one of the pathological features of NDPH. The change of morphological similarity between the right superior frontal gyrus and right hippocampus further reflects the cognitive impairment on brain structure. These observations hold great implications for the prediction of clinical characteristics in NDPH, contributing

to further advancements in neuroscience research and clinical diagnostics.

Abbreviations

AAL	Anatomical automatic labeling
Anat-SFSeg	Anatomically-guided superficial fiber segmentation
AF	Arcuate fasciculus
AD	Axial diffusivity
BMI	Body mass index
DWM	Deep white matter
dMRI	Diffusion magnetic resonance imaging
DTI	Diffusion tensor imaging
DTI-ALPS	Diffusion tensor imaging along the perivascular space
TE	Echo time
FOD	Fiber orientation distribution
FSL	Oxford Centre for Functional MRI of the Brain's Software Library
FA	Fractional anisotropy
GAD-7	Generalized Anxiety Disorder-7
HIT-6	Headache Impact Test-6
HC	Healthy control
TI	Inversion time
MPRAGE	Magnetization-prepared rapid gradient echo
MD	Mean diffusivity
MoCA	Montreal Cognitive Assessment
MRI	Magnetic resonance imaging
NBS	Network-based statistic
NDPH	New daily persistent headache
ORG	O'Donnell Research Group
FMRIB	Oxford Centre for Functional MRI of the Brain
PHQ-9	Patient Health Questionnaire-9
PSQI	Pittsburgh Sleep Quality Index
RD	Radial diffusivity
R2SN	Regional radiomics similarity networks
TR	Repetition time
SF	Striato-frontal
SCN	Structural covariance network
SWM	Superficial white matter
Sup-F	Superficial-frontal
Sup-O	Superficial-occipital
Sup-OT	Superficial-occipital-temporal
Sup-T	Superficial-temporal
SLF	Superior longitudinal fasciculus
T1w	T1-weighted
TO	Thalamo-occipital
TBSS	Tract-based spatial statistics
UF	Uncinate fasciculus
VAS	Visual Analogue Scale

Supplementary Information

The online version contains supplementary material available at https://doi.org/10.1186/s10194-024-01899-9.

Supplementary Material 1

Acknowledgements

We extend our sincere gratitude to the National Neurological Imaging Centre of Beijing Tiantan Hospital, Capital Medical University, for their invaluable technical and equipment support throughout this study. Additionally, we express our heartfelt appreciation to the headache specialists whose expertise was instrumental in ensuring accurate diagnoses.

Author contributions

The study was conceptualized and designed by DZ, YLM, KZ, FRZ, BBS and YGW. BBS, YGW, and FRZ provided supervision and guidance throughout the study. DZ and YLM conducted the initial data analysis. YLM and DQ oversaw data quality control measures. All authors participated in clinical and MRI data collection. DZ and YLM drafted the initial manuscript, which was critically reviewed and revised by all authors until consensus on the final version was reached.

Funding

The research presented in this study was funded by the Beijing Natural Science Foundation (grant numbers Z200024 and 7244519), the National Natural Science Foundation of China (grant numbers 32170752, 31770800, 91849104 and 82371910), and supported by BUPT Excellent Ph.D. Students Foundation (grant number CX20241085).

Data availability

The datasets used and analyzed during the current study are available from the corresponding author on reasonable request.

Declarations

Ethics approval and consent to participate

Every participant was provided with comprehensive information regarding the study, and they voluntarily signed an informed consent form. In addition to being registered on Clinical Trial (NCT05334927), our research was also granted ethical approval by Beijing Tiantan Hospital, Capital Medical University (no. KY2022-044).

Consent for publication

All authors consent for the publication.

Competing interests

The authors declare no competing interests.

Author details

[1]School of Artificial Intelligence, Beijing University of Posts and Telecommunications, No.10 Xitucheng Road, Haidian District, Beijing 100876, China
[2]Headache Center, Department of Neurology, Beijing Tiantan Hospital, Capital Medical University, No.119 South Fourth Ring West Road, Fengtai District, Beijing 100070, China
[3]Tiantan Neuroimaging Center for Excellence, China National Clinical Research Center for Neurological Diseases, Beijing Neurosurgical Institute, Beijing Tiantan Hospital, Capital Medical University, No.119 South Fourth Ring West Road, Fengtai District, Beijing 100070, China
[4]Department of Neurology, The First Affiliated Hospital of Dalian Medical University, No.222 Zhongshan Road, Xigang District, Dalian, Liaoning 116011, China
[5]Queen Mary School Hainan, Beijing University of Posts and Telecommunications, Hainan Lingshui Li'an International Education Innovation Pilot Zone, Lingshui, Hainan 572426, China

Received: 19 September 2024 / Accepted: 25 October 2024
Published online: 04 November 2024

References

1. Headache Classification Committee of the International Headache Society (IHS) The International Classification of Headache Disorders, 3rd edition. Cephalalgia (2018);38(1):1–211. https://doi.org/10.1177/0333102417738202
2. Gelfand AA, Robbins MS, Szperka CL (2022) New Daily Persistent Headache-A Start with an Uncertain End. JAMA Neurol 79(8):733–734. https://doi.org/10.1001/jamaneurol.2022.1727
3. Aaseth K, Grande RB, Kvårner KJ (2008) Prevalence of secondary chronic headaches in a population-based sample of 30-44-year-old persons. The Akershus study of chronic headache. Cephalalgia 28(7):705–713. https://doi.org/10.1111/j.1468-2982.2008.01577.x
4. Yamani N, Olesen J (2019) New daily persistent headache: a systematic review on an enigmatic disorder. J Headache Pain 20(1):80. https://doi.org/10.1186/s10194-019-1022-z
5. Ashina M (2020) Migraine. N Engl J Med 383(19):1866–1876. https://doi.org/10.1056/NEJMra1915327
6. Davis KD, Flor H, Greely HT et al (2017) Brain imaging tests for chronic pain: medical, legal and ethical issues and recommendations. Nat Rev Neurol 13(10):624–638. https://doi.org/10.1038/nrneurol.2017.122
7. Peng KP, Rozen TD (2023) Update in the understanding of new daily persistent headache. Cephalalgia 43(2). https://doi.org/10.1177/03331024221146314

8. Schwedt TJ, Chiang CC, Chong CD et al (2015) Functional MRI of migraine. Lancet Neurol 14(1):81–91. https://doi.org/10.1016/s1474-4422(14)70193-0
9. Planchuelo-Gómez Á, García-Azorín D, Guerrero ÁL et al (2020) White matter changes in chronic and episodic migraine: a diffusion tensor imaging study. J Headache Pain 21(1):1. https://doi.org/10.1186/s10194-019-1071-3
10. Peng KP, Wang SJ (2022) Update of New Daily Persistent Headache. Curr Pain Headache Rep 26(1):79–84. https://doi.org/10.1007/s11916-022-01005-1
11. Cheema S, Mehta D, Ray JC et al (2023) New daily persistent headache: A systematic review and meta-analysis. Cephalalgia 43(5):3331024231168089. https://doi.org/10.1177/03331024231168089
12. Szabo E, Chang YC, Shulman J et al (2022) Alterations in the structure and function of the brain in adolescents with new daily persistent headache: A pilot MRI study. Headache 62(7):858–869. https://doi.org/10.1111/head.14360
13. Qiu D, Wang W, Mei Y et al (2023) Brain structure and cortical activity changes of new daily persistent headache: multimodal evidence from MEG/sMRI. J Headache Pain 24(1):45. https://doi.org/10.1186/s10194-023-01581-6
14. Mei Y, Wang W, Qiu D et al (2023) Micro-structural white matter abnormalities in new daily persistent headache: a DTI study using TBSS analysis. J Headache Pain 24(1):80. https://doi.org/10.1186/s10194-023-01620-2
15. Zhang X, Wang W, Zhang X et al (2023) Normal glymphatic system function in patients with new daily persistent headache using diffusion tensor image analysis along the perivascular space. Headache 63(5):663–671. https://doi.org/10.1111/head.14514
16. Seidlitz J, Váša F, Shinn M et al (2018) Morphometric similarity networks detect microscale cortical organization and predict inter-individual cognitive variation. Neuron 97(1):231–247e7. https://doi.org/10.1016/j.neuron.2017.11.039
17. Pfefferbaum A, Sullivan EV (2003) Increased brain white matter diffusivity in normal adult aging: relationship to anisotropy and partial voluming. Magn Reson Med 49(5):953–961. https://doi.org/10.1002/mrm.10452
18. Guevara M, Guevara P, Román C et al (2020) Superficial white matter: A review on the dMRI analysis methods and applications. Neuroimage 212:116673. https://doi.org/10.1016/j.neuroimage.2020.116673
19. Phillips OR, Joshi SH, Squitieri F et al (2016) Major Superficial White Matter Abnormalities in Huntington's Disease. Front Neurosci 10:197. https://doi.org/10.3389/fnins.2016.00197
20. Phillips OR, Joshi SH, Piras F et al (2016) The superficial white matter in Alzheimer's disease. Hum Brain Mapp 37(4):1321–1334. https://doi.org/10.1002/hbm.23105
21. Zhang D, Zong F, Zhang Q et al (2024) Anat-SFSeg: Anatomically-guided superficial fiber segmentation with point-cloud deep learning. Med Image Anal 95:103165. https://doi.org/10.1016/j.media.2024.103165
22. Carlsson AM (1983) Assessment of chronic pain. I. Aspects of the reliability and validity of the visual analogue scale. Pain 16(1):87–101. https://doi.org/10.1016/0304-3959(83)90088-X
23. Bayliss MS, Dewey JE, Dunlap I et al (2003) A study of the feasibility of Internet administration of a computerized health survey: The Headache Impact Test (HIT). Qual Life Res 12:953–961. https://doi.org/10.1023/A:1026167214355
24. Negeri ZF, Levis B, Sun Y et al (2021) Accuracy of the Patient Health Questionnaire-9 for screening to detect major depression: updated systematic review and individual participant data meta-analysis. BMJ 375:n2183. https://doi.org/10.1136/bmj.n2183
25. Löwe B, Decker O, Müller S et al (2008) Validation and standardization of the Generalized Anxiety Disorder Screener (GAD-7) in the general population. Med Care 46(3):266–274. https://doi.org/10.1097/MLR.0b013e318160d093
26. Li J, Yao YS, Dong Q et al (2013) Characterization and factors associated with sleep quality among rural elderly in China. Arch Gerontol Geriatr 56(1):237–243. https://doi.org/10.1016/j.archger.2012.08.002
27. Nasreddine ZS, Phillips NA, Bédirian V et al (2005) The Montreal Cognitive Assessment, MoCA: a brief screening tool for mild cognitive impairment. J Am Geriatr Soc 53(4):695–699. https://doi.org/10.1111/j.1532-5415.2005.53221.x
28. Zhao K, Zheng Q, Che T et al (2021) Regional radiomics similarity networks (R2SNs) in the human brain: reproducibility, small-world properties and a biological basis. Netw Neurosci 5(3):783–797. https://doi.org/10.1162/netn_a_00200
29. Tournier JD, Smith R, Raffelt D et al (2019) MRtrix3: A fast, flexible and open software framework for medical image processing and visualisation. Neuroimage 202:116137. https://doi.org/10.1016/j.neuroimage.2019.116137
30. Veraart J, Novikov DS, Christiaens D et al (2016) Denoising of diffusion MRI using random matrix theory. Neuroimage 142:394–406. https://doi.org/10.1016/j.neuroimage.2016.08.016
31. Kellner E, Dhital B, Kiselev VG et al (2016) Gibbs-ringing artifact removal based on local subvoxel-shifts. Magn Reson Med 76:1574–1581. https://doi.org/10.1002/mrm.26054
32. Andersson JL, Sotiropoulos SN (2015) An integrated approach to correction for off-resonance effects and subject movement in diffusion MR imaging. Neuroimage 125:1063–1078. https://doi.org/10.1016/j.neuroimage.2015.10.019
33. Smith SM, Jenkinson M, Woolrich MW et al (2004) Advances in functional and structural MR image analysis and implementation as FSL. Neuroimage 23:S208–S219. https://doi.org/10.1016/j.neuroimage.2004.07.051
34. Skare S, Bammer R (2010) Jacobian weighting of distortion corrected EPI data. Proceedings of the International Society for Magnetic Resonance in Medicine, 5063
35. Andersson JL, Skare S, Ashburner J (2003) How to correct susceptibility distortions in spin-echo echo-planar images: application to diffusion tensor imaging. Neuroimage 20:870–888. https://doi.org/10.1016/S1053-8119(03)00336-7
36. Tustison N, Avants B, Cook P et al (2010) N4ITK: Improved N3 Bias Correction. IEEE Trans Med Imaging 29:1310–1320. https://doi.org/10.1109/TMI.2010.2046908
37. Basser PJ, Mattiello J, LeBihan D (1994) Estimation of the effective self-diffusion tensor from the NMR spin echo. J Magn Reson B 103:247–254. https://doi.org/10.1006/jmrb.1994.1037
38. Veraart J, Sijbers J, Sunaert S et al (2013) Weighted linear least squares estimation of diffusion MRI parameters: strengths, limitations, and pitfalls. Neuroimage 81:335–346. https://doi.org/10.1016/j.neuroimage.2013.05.028
39. Smith SM (2002) Fast robust automated brain extraction. Hum Brain Mapp 17(3):143–155. https://doi.org/10.1002/hbm.10062
40. Jenkinson M, Beckmann CF, Behrens TE et al (2012) FSL Neuroimage 62(2):782–790. https://doi.org/10.1016/j.neuroimage.2011.09.015
41. Zhang F, Wu Y, Norton I et al (2018) An anatomically curated fiber clustering white matter atlas for consistent white matter tract parcellation across the lifespan. Neuroimage 179:429–447. https://doi.org/10.1016/j.neuroimage.2018.06.027
42. Avants BB, Tustison N, Song G (2009) Advanced normalization tools (ANTS). Insight j 2(365):1–35
43. Desikan RS, S´egonne F, Fischl B et al (2006) An automated labeling system for subdividing the human cerebral cortex on mri scans into gyral based regions of interest. Neuroimage 31(3):968–980. https://doi.org/10.1016/j.neuroimage.2006.01.021
44. Fischl B, Salat DH, Busa E et al (2002) Whole brain segmentation: automated labeling of neuroanatomical structures in the human brain. Neuron 33(3):341–355. https://doi.org/10.1016/s0896-6273(02)00569-x
45. Fischl B, Van Der Kouwe A, Destrieux C et al (2004) Automatically parcellating the human cerebral cortex. Cereb Cortex 14(1):11–22. https://doi.org/10.1093/cercor/bhg087
46. Fischl B (2012) FreeSurfer Neuroimage 62(2):774–781. https://doi.org/10.1016/jneuroimage.2012.01.021
47. Tournier JD, Calamante F, Connelly A (2007) Robust determination of the fibre orientation distribution in diffusion MRI: non-negativity constrained super-resolved spherical deconvolution. Neuroimage 35(4):1459–1472. https://doi.org/10.1016/j.neuroimage.2007.02.016
48. Tournier JD, Calamante F, Connelly A (2010) Improved probabilistic streamlines tractography by 2nd order integration over fibre orientation distributions. Proceedings of the International Society for Magnetic Resonance in Medicine, 1670
49. O'Donnell LJ, Wells WM, Golby AJ et al (2012) Unbiased groupwise registration of white matter tractography. Med Image Comput Comput Assist Interv 15(Pt 3):123–130. https://doi.org/10.1007/978-3-642-33454-2_16
50. Fischl B (2012) FreeSurfer Neuroimage 62(2):774–781. https://doi.org/10.1016/j.neuroimage.2012.01.021
51. Xue T, Zhang F, Zhang C et al (2023) Superficial white matter analysis: An efficient point-cloud-based deep learning framework with supervised contrastive learning for consistent tractography parcellation across populations and dMRI acquisitions. Med Image Anal 85:102759. https://doi.org/10.1016/j.media.2023.102759
52. Tzourio-Mazoyer N, Landeau B, Papathanassiou D et al (2002) Automated anatomical labeling of activations in SPM using a macroscopic anatomical parcellation of the MNI MRI single-subject brain. Neuroimage 15(1):273–289. https://doi.org/10.1006/nimg.2001.0978

53. Aerts HJ, Velazquez ER, Leijenaar RT et al (2014) Decoding tumour phenotype by noninvasive imaging using a quantitative radiomics approach. Nat Commun 5:4006. https://doi.org/10.1038/ncomms5006
54. Feng F, Wang P, Zhao K et al (2018) Radiomic Features of Hippocampal Subregions in Alzheimer's Disease and Amnestic Mild Cognitive Impairment. Front Aging Neurosci 10:290. https://doi.org/10.3389/fnagi.2018.00290
55. Zhao K, Ding Y, Han Y et al (2020) Independent and reproducible hippocampal radiomic biomarkers for multisite Alzheimer's disease: diagnosis, longitudinal progress and biological basis. Sci Bull 65(13):1103–1113. https://doi.org/10.1016/j.scib.2020.04.003
56. Van Griethuysen JJM, Fedorov A, Parmar C et al (2017) Computational Radiomics System to Decode the Radiographic Phenotype. Cancer Res 77(21):e104–e107. https://doi.org/10.1158/0008-5472.Can-17-0339
57. Zalesky A, Fornito A, Bullmore ET (2010) Network-based statistic: identifying differences in brain networks. Neuroimage 53(4):1197–1207. https://doi.org/10.1016/j.neuroimage.2010.06.041
58. Wang J, Wang X, Xia M et al (2015) GRETNA: a graph theoretical network analysis toolbox for imaging connectomics. Front Hum Neurosci 9:386. https://doi.org/10.3389/fnhum.2015.00386
59. Loh WY (2011) Classification and regression trees. Wires Data Min Knowl 1(1):14–23. https://doi.org/10.1002/widm.8
60. Song SK, Sun SW, Ramsbottom MJ et al (2002) Dysmyelination revealed through MRI as increased radial (but unchanged axial) diffusion of water. Neuroimage 17(3):1429–1436. https://doi.org/10.1006/nimg.2002.1267
61. Alexander AL, Lee JE, Lazar M et al (2007) Diffusion tensor imaging of the brain. Neurotherapeutics 4(3):316–329. https://doi.org/10.1016/j.nurt.2007.05.011
62. Jones DK, Knösche TR, Turner R (2013) White matter integrity, fiber count, and other fallacies: the do's and don'ts of diffusion MRI. Neuroimage 73:239–254. https://doi.org/10.1016/j.neuroimage.2012.06.081
63. Wang R, Dong Z, Chen X et al (2014) Cognitive processing of cluster headache patients: evidence from event-related potentials. J Headache Pain 15:1–7. https://doi.org/10.1186/1129-2377-15-66
64. Cheng K, Martin LF, Slepian MJ et al (2021) Mechanisms and Pathways of Pain Photobiomodulation: A Narrative Review. J Pain 22(7):763–777. https://doi.org/10.1016/j.jpain.2021.02.005
65. Ayoub LJ, Barnett A, Leboucher A et al (2019) The medial temporal lobe in nociception: a meta-analytic and functional connectivity study. Pain 160(6):1245–1260. https://doi.org/10.1097/j.pain.0000000000001519
66. Vos SB, Jones DK, Jeurissen B et al (2012) The influence of complex white matter architecture on the mean diffusivity in diffusion tensor MRI of the human brain. Neuroimage 59(3):2208–2216. https://doi.org/10.1016/j.neuroimage.2011.09.086
67. Antoine LH, Tanner JJ, Mickle AM et al (2023) Greater socioenvironmental risk factors and higher chronic pain stage are associated with thinner bilateral temporal lobes. Brain Behav 13(12):e3330. https://doi.org/10.1002/brb3.3330
68. Yuan Z, Wang W, Zhang X et al (2022) Altered functional connectivity of the right caudate nucleus in chronic migraine: a resting-state fMRI study. J Headache Pain 23(1):154. https://doi.org/10.1186/s10194-022-01506-9
69. Wang N, Zhang YH, Wang JY et al (2021) Current Understanding of the Involvement of the Insular Cortex in Neuropathic Pain: A Narrative Review. Int J Mol Sci 22(5):2648. https://doi.org/10.3390/ijms22052648
70. Walker L, Gozzi M, Lenroot R et al (2012) Diffusion tensor imaging in young children with autism: biological effects and potential confounds. Biol Psychiatry 72(12):1043–1051. https://doi.org/10.1016/j.biopsych.2012.08.001
71. Boisgueheneuc F, Levy R, Volle E et al (2006) Functions of the left superior frontal gyrus in humans: a lesion study. Brain 129(12):3315–3328. https://doi.org/10.1093/brain/awl244
72. Moser MB, Moser EI (1998) Functional differentiation in the hippocampus. Hippocampus 8(6): 608–619. https://doi.org/10.1002/(SICI)1098-1063(1998)8:6<608::AID-HIPO3>3.0.CO;2-7
73. Zhao K, Chen P, Alexander-Bloch A et al (2023) A neuroimaging biomarker for Individual Brain-Related Abnormalities In Neurodegeneration (IBRAIN): a cross-sectional study. EClinicalMedicine 65:102276. https://doi.org/10.1016/j.eclinm.2023.102276
74. Zhao K, Zheng Q, Dyrba M et al (2022) Regional radiomics similarity networks reveal distinct subtypes and abnormality patterns in mild cognitive impairment. Adv Sci 9(12):2104538. https://doi.org/10.1002/advs.202104538
75. Zhao K, Wang D, Wang D et al (2024) Macroscale connectome topographical structure reveals the biomechanisms of brain dysfunction in Alzheimer's disease. Sci Adv 10(41):eado8837. https://doi.org/10.1126/sciadv.ado8837

Publisher's note